

Electronic Supporting information (ESI)

**Charge-transfer-featured materials—promising hosts for
fabrication of efficient OLED through triplet harvesting via
triplet fusion**

Jie Zhou,^{a‡} Ping Chen,^{b‡} Xu Wang,^{c‡} Yan Wang,^d Yi Wang,^a Feng Li,^{b*}
Minghui Yang,^d Yan Huang,^a Junsheng Yu,^{c*} and Zhiyun Lu^{a*}

^aKey Laboratory of Green Chemistry and Technology (Ministry of Education), College of Chemistry, Sichuan University, Chengdu 610064, PR China. E-mail: luzhiyun@scu.edu.cn

^bState Key Laboratory of Supramolecular Structure and Materials, Jilin University, Changchun 130012, PR China. E-mail: lifeng01@jlu.edu.cn

^cSchool of Optoelectronic Information, University of Electronic Science and Technology of China (UESTC), Chengdu 610054, PR China. E-mail: jsyu@uestc.edu.cn

^dKey Laboratory of Magnetic Resonance in Biological Systems, State Key Laboratory of Magnetic Resonance and Atomic/Molecular Physics, Wuhan Institute of Physics and Mathematics, Chinese Academy of Sciences, Wuhan 430071, PR China.

Contents

1	Photophysical, electrochemical, and electroluminescent characteristics	S2
2	Experimental details	S12
3	¹ H NMR, ¹³ C NMR, FT-IR and HRMS spectra of the objective compound	S20

1 Photophysical, electrochemical, and electroluminescent characteristics

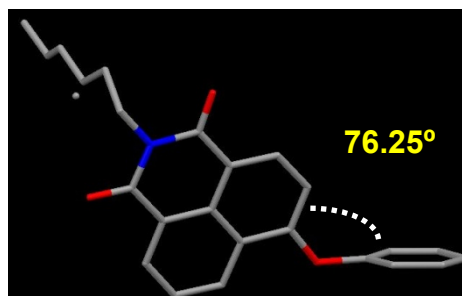
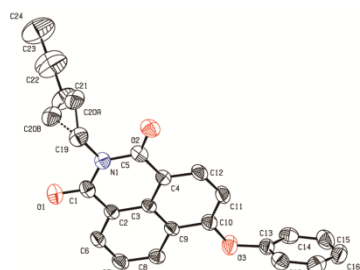


Fig. S1 ORTEP plot of the structure of **PhONI** (hydrogen atoms removed for clarity, ellipsoids at 30% probability).

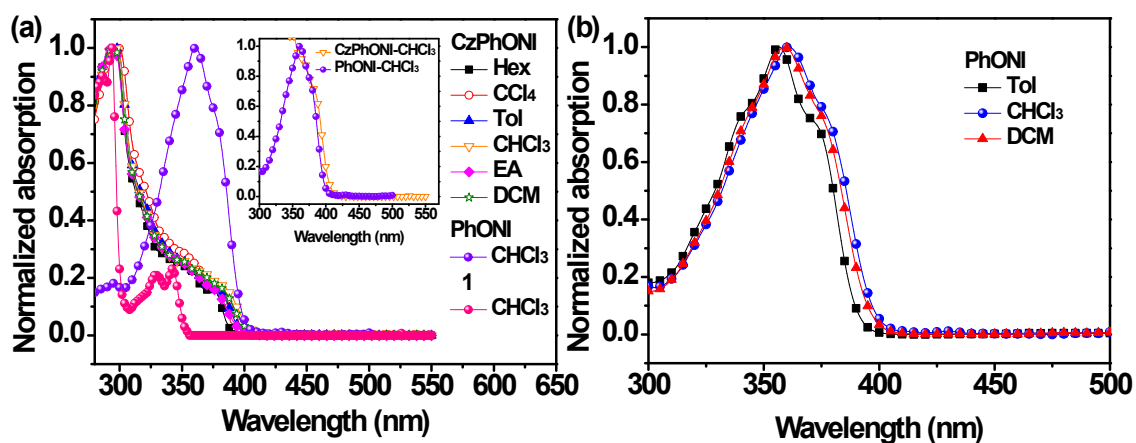


Fig. S2 UV-Vis absorption spectra of: (a) **CzPhONI** (10^{-5} M) in solvents with different polarities, compound **1** (9-(4-*t*-butylphenyl)-9*H*-carbazole) and **PhONI** in chloroform (10^{-5} M) (inset: the overlap of UV-Vis spectra between **CzPhONI** and **PhONI** at low energy region); (b) **PhONI** (10^{-5} M) in solvents with different polarities.

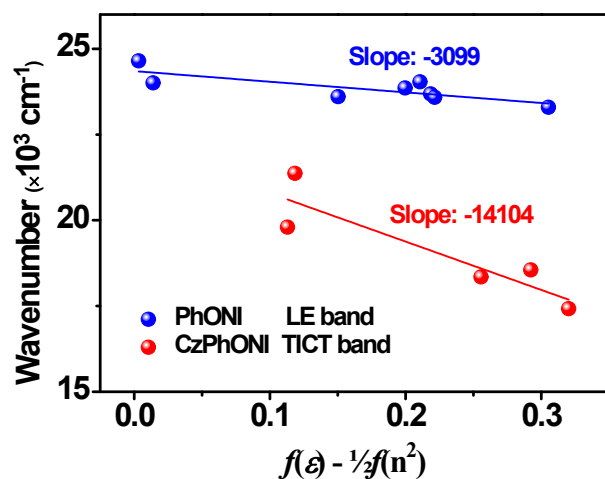


Fig. S3 The Lippert-Mataga plot of the wave number of the emission maxima $\nu_{\text{p}}^{\text{max}}$ of **CzPhONI** and **PhONI** versus solvent polarity parameters. For the LE emission bands, the solvent polarity parameter $f(\epsilon-n) = f(\epsilon) - f(n^2)$; while for the TICT emission bands, $f(\epsilon-n) = f(\epsilon) - 1/2f(n^2)$.¹

$$\text{Here, } f(\epsilon) = \frac{(\epsilon - 1)}{(2\epsilon + 1)}; \quad f(n^2) = \frac{(n^2 - 1)}{(2n^2 + 1)}$$

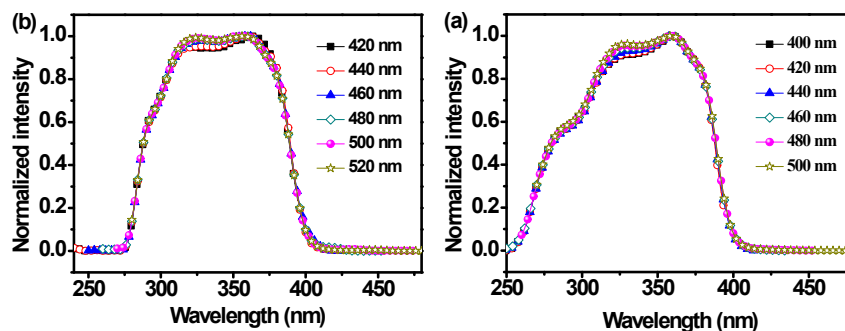


Fig. S4 Normalized excitation spectra of 10^{-5} M solution of **CzPhONI** in (a) Tol, and (b) CCl_4 at different emission wavelengths.

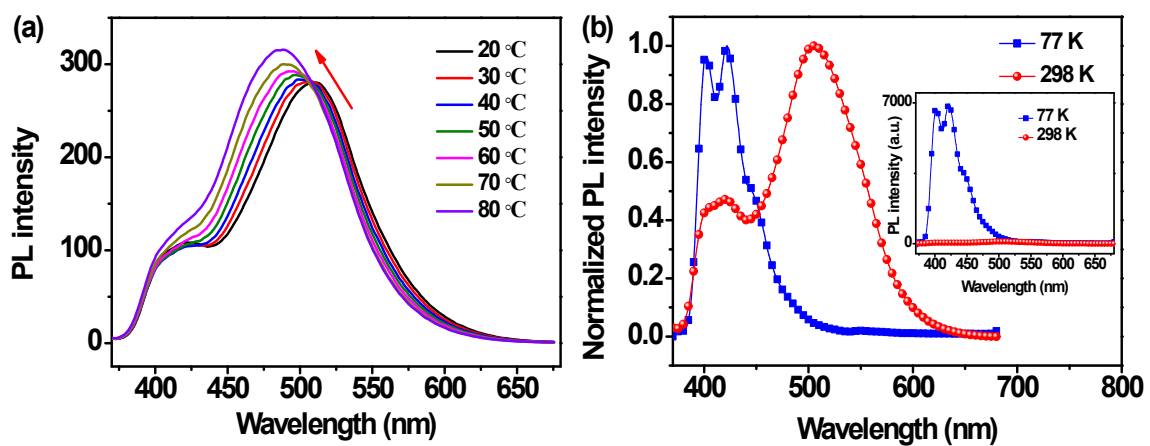


Fig. S5 (a) Changes on PL spectrum of **CzPhONI** as a function of temperature in Tol (10^{-5} M). (b) Normalized fluorescence spectra of **CzPhONI** in Tol (10^{-6} M) measured at 298 K and 77 K, respectively.

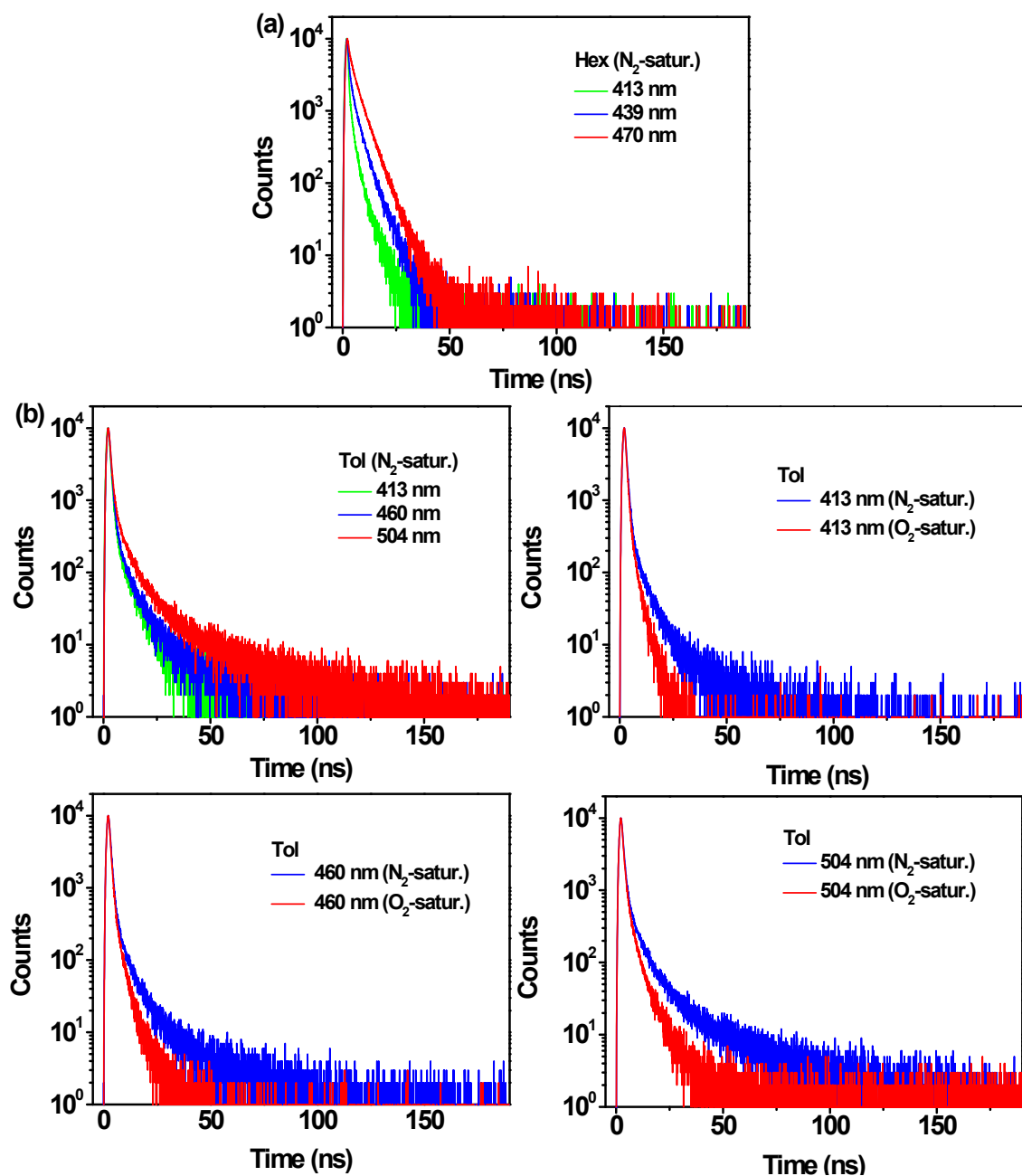


Fig. S6 The fluorescence decay curves of CzPhONI (10^{-6} M) at different emission bands in (a) N_2 -saturated Hex; and (b) N_2 -saturated and O_2 -saturated Tol.

Table S1 The fluorescence life time data of **CzPhONI** at different emission wavelengths in N₂-saturated Hex, N₂-saturated Tol, and O₂-saturated Tol (10⁻⁶ M)

Solvent	λ_{em} (nm)	Life time (ns)	Content (%)	χ^2
Hex-N ₂ saturated	413	$\tau_1 = 0.11$	66.8	1.02
		$\tau_2 = 1.25$	22.7	
		$\tau_3 = 4.41$	10.5	
	439	$\tau_1 = 0.16$	36.9	0.95
		$\tau_2 = 1.62$	28.9	
		$\tau_3 = 5.05$	34.2	
470	$\tau_1 = 0.27$	14.4	1.01	
	$\tau_2 = 2.28$	29.0		
	$\tau_3 = 5.40$	56.6		
Tol-N ₂ saturated	413	$\tau_1 = 0.79$	83.9	1.06
		$\tau_2 = 3.64$	12.7	
		$\tau_3 = 12.47$	3.4	
	460	$\tau_1 = 0.87$	82.9	1.01
		$\tau_2 = 4.47$	14.1	
		$\tau_3 = 21.48$	3.0	
504	$\tau_1 = 0.88$	71.4	1.14	
	$\tau_2 = 4.83$	21.9		
	$\tau_3 = 22.98$	6.7		
Tol-O ₂ saturated	413	$\tau_1 = 0.12$	26.6	1.06
		$\tau_2 = 0.80$	63.4	
		$\tau_3 = 3.20$	10.0	
	460	$\tau_1 = 0.71$	76.3	1.04
		$\tau_2 = 1.93$	18.0	
		$\tau_3 = 5.14$	5.7	
504	$\tau_1 = 0.70$	66.1	1.02	
	$\tau_2 = 2.24$	25.7		
	$\tau_3 = 6.75$	8.2		

Table S2 Photophysical properties of **PhONI** and **CzPhONI** (10^{-6} M) in solvents of different polarities

Solvent	PhONI			CzPhONI		
	$\lambda_{\text{abs}}^{\text{a}}$ (nm)	$\lambda_{\text{PL}}^{\text{b}}$ (nm)	PL QY ^c	$\lambda_{\text{abs}}^{\text{a}}$ (nm)	$\lambda_{\text{PL}}^{\text{b}}$ (nm)	PL QY ^c
CHX	354	406	0.86	-	-	-
Hex	-	-	-	296	394, 413, 439	0.025
CCl ₄	-	-	-	299	409, 428, 468	0.024
Tol	358	418	0.87	296	413, 504	0.012
CHCl ₃	363	428	0.78	296	414, 542	0.002
EA	357	418	0.82	295	406, 541	0.002
DCM	361	428	0.86	296	403, 575	0.002
Film	-	-	-	298	493	0.082

^a λ_{abs} : absorption maximum; ^b λ_{em} : fluorescence maximum; ^c PL QY: photoluminescence quantum yield.

CHX denotes cyclohexane; Hex denotes *n*-hexane; Tol denotes toluene; EA denotes ethyl acetate; DCM denotes dichloromethane.

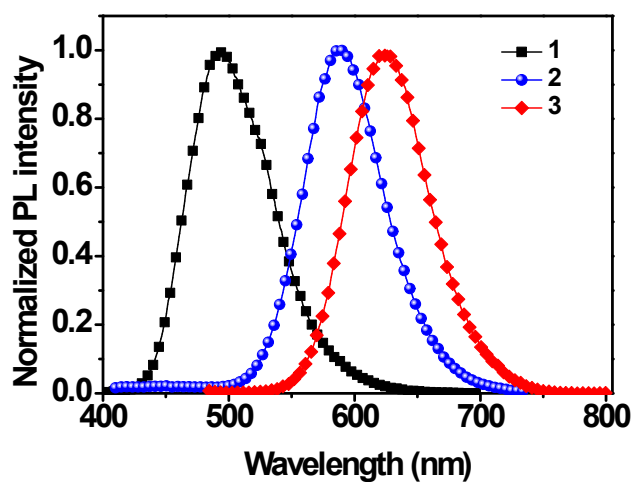


Fig. S7 PL spectra of thin film samples of **CzPhONI** (1), **FN1b** blended into **CzPhONI** with concentration of 6 wt% (2), and **FN1b** (3).

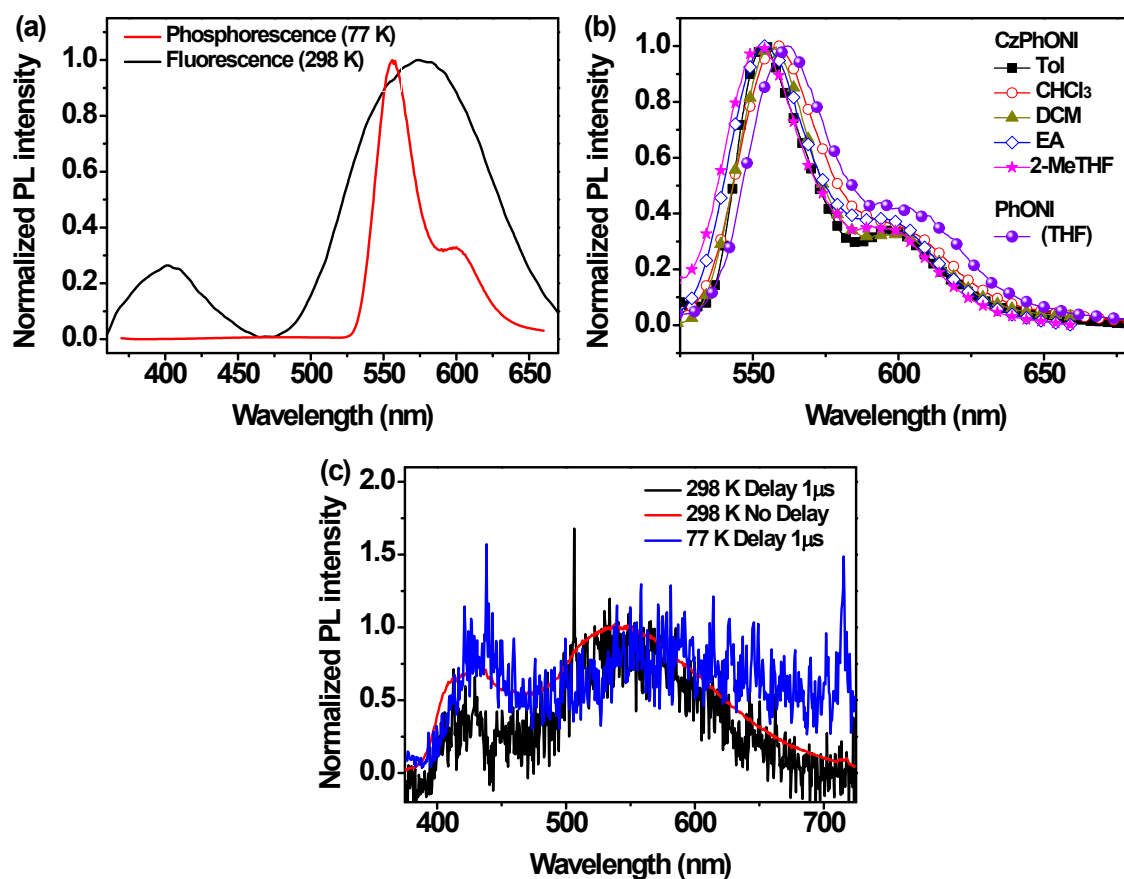


Fig. S8 (a) Fluorescence spectrum of **CzPhONI** in DCM (10^{-6} M) at 298 K, and phosphorescence spectrum at 77 K in DCM. (10^{-6} M) (b) Phosphorescence spectra of **CzPhONI** and **PhONI** at 77 K in various solvents. (c) Transient PL characteristics of **CzPhONI** (10^{-6} M) in tetrahydrofuran.

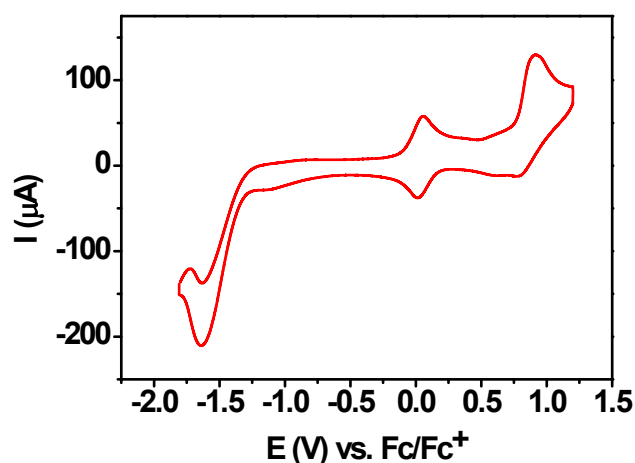


Fig S9. The cyclic voltametric voltammogram of thin film sample of **CzPhONI**. The redox potentials are determined relative to Ag/Ag^+ in acetonitrile, using Fc/Fc^+ as internal reference.

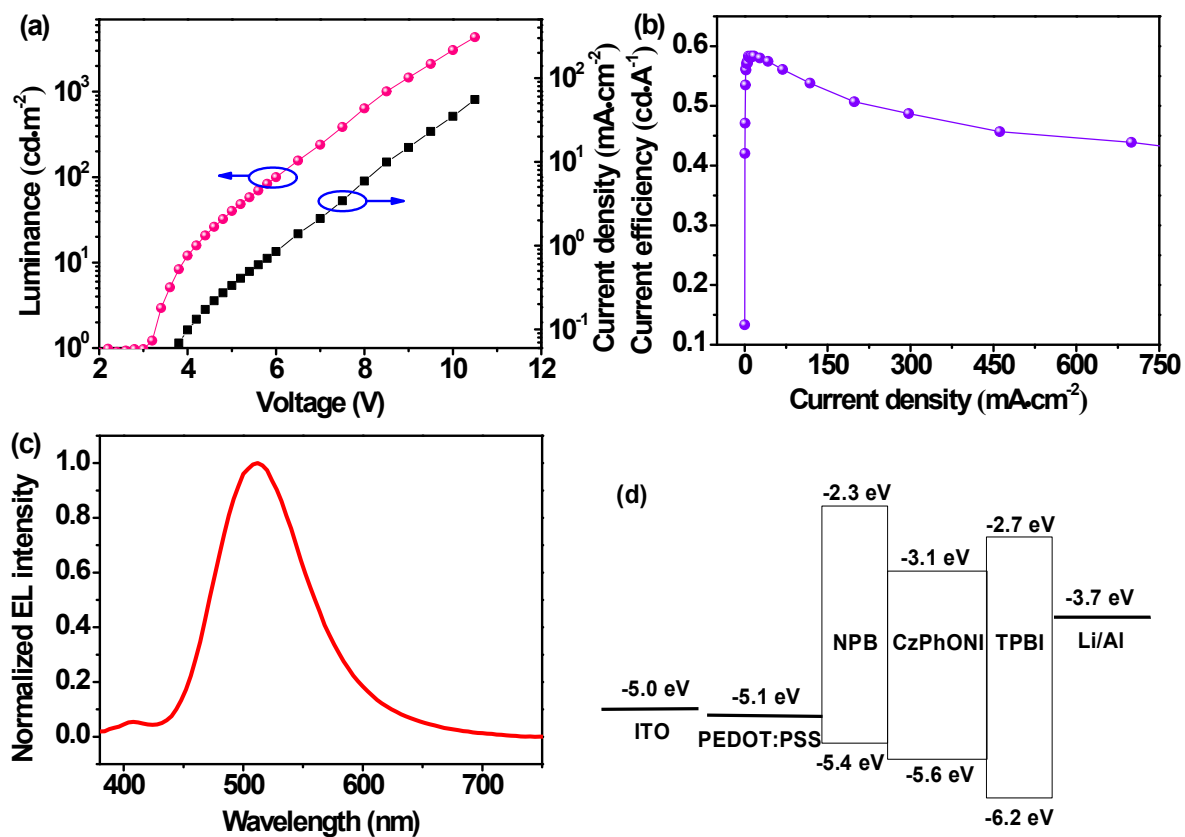


Fig. S10 Current density-voltage-luminescence curves (a), current efficiency-current density curve (b), normalized EL spectrum at 8 V(c), and energy level diagram (d) of Device I.

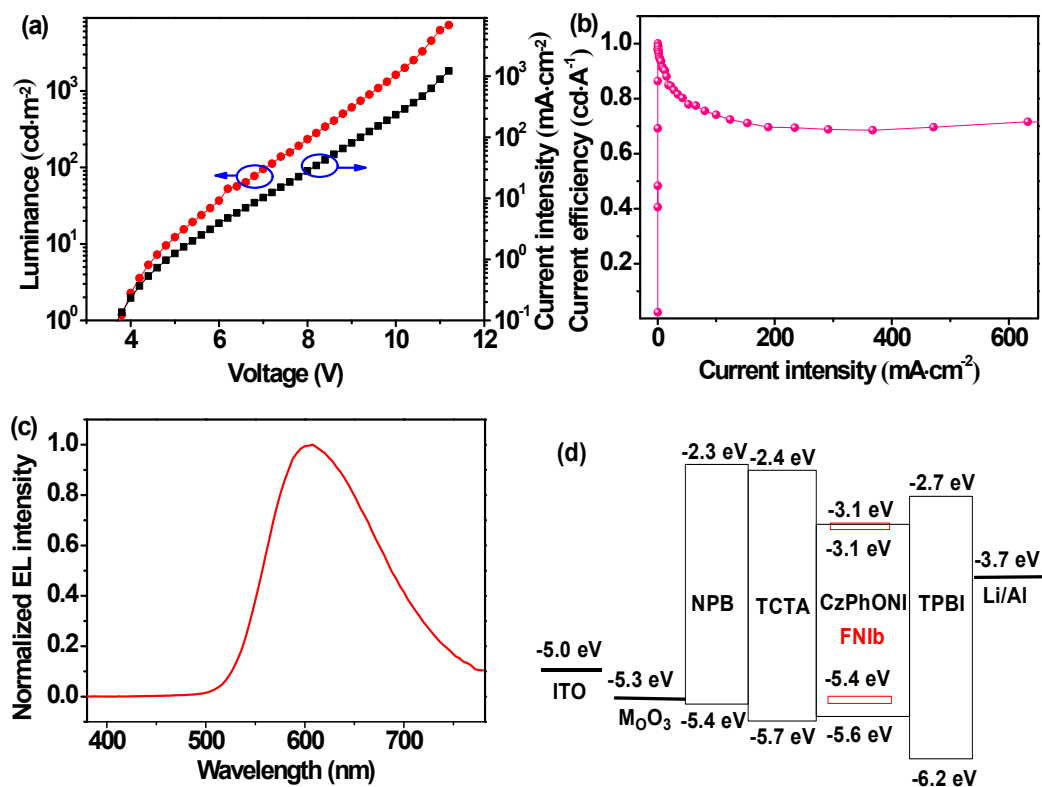


Fig. S11 Current density-voltage-luminescence curves (a), current efficiency-current density curve (b), normalized EL spectrum at 8 V (c), and energy level diagram (d) of Device II.

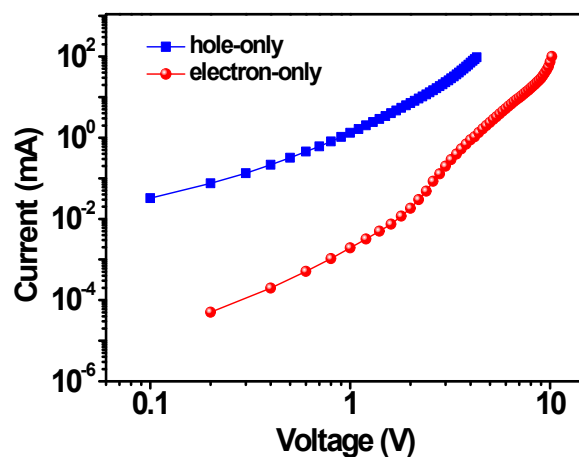


Fig. S12 Current density-voltage characteristics of the hole-only and electron-only devices of CzPhONI.

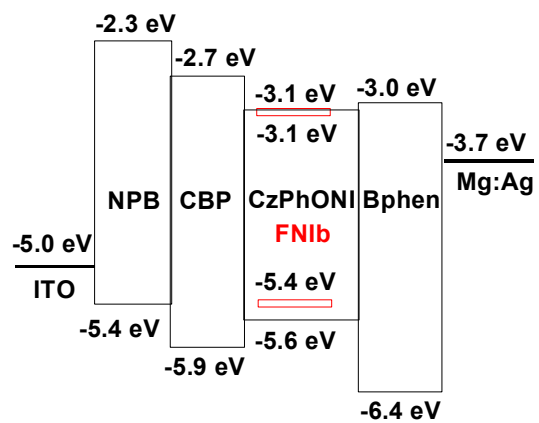


Fig. S13 Energy level diagram of Device III.

2 Experimental details.

1) General

All the chemicals and reagents involved in the synthetic procedure were commercially available and were used without purification unless otherwise stated. All solvents were of analytical grades and distilled freshly prior to use according to the standard procedures. The reference compound **PhONI** was synthesized according to literature ² with yield of 78%.

N,N'-bis(1-naphyl)-*N,N'*-diphenyl-1,1'-biphenyl-4,4'-diamine (NPB), 4,4',4''-tris(*N*-carbazyl)triphenylamine (TCTA), 4,4'-bis(9-carbazyl)biphenyl (CBP), 4,7-diphenyl-1,10-phenanthroline (BPhen), 2',2''-(1,3,5-benzinetriyl)-tris(1-phenyl-1*H*-benzimidazole) (TPBI) are purchased from Lumtec. Co. NPB and TCTA functioned as hole-transporting materials, CBP as hole-blocking material, while BPhen and TPBI functioned as electron-transporting materials in the OLEDs.

¹H NMR and ¹³C NMR spectra were measured on a Bruker AVII-400 spectrometer in CDCl₃ using TMS as internal standard. High resolution MS spectra were recorded on a Water Q-TOF-Premier instrument. FT-IR spectra were recorded on a Perkin-Elmer 2000 infrared spectrometer with KBr pellets under an ambient atmosphere. The determination of the unit cell and data collection for the single crystal sample of **PhONI** were performed on a Xcalibur E X-ray single crystal diffractometer equipped with graphite monochromator Mo K α ($\lambda = 0.71073 \text{ \AA}$) radiation. The data collection was executed using CrysAlisPro program. Structure was solved by direct method and successive Fourier difference syntheses (SHELXS-97), and was refined by full-matrix least-squares procedure on F^2 with anisotropic thermal parameters for all non-hydrogen atoms (SHELXL-97). The PL emission spectra of both solution and thin-film samples were determined on a PerkinElmer LS55 fluorescence spectrophotometer. PL QYs in dilute solution were determined using quinine sulfate in 0.05 mol·L⁻¹ H₂SO₄ ($\phi = 0.55$) as standard under excitation of

350 nm; while absolute PL QYs of thin film were determined on a Horiba Jobin Yvon-Edison Fluoromax-4 fluorescence spectrometer equipped with an integrating sphere (IS80 from Labsphere) and digital photometer (S370 from UDT) under ambient conditions. The transient photoluminescence decay characteristics of the pre-degassed solution samples were recorded on a Single Photon Counting Controller FluoroHub-B. The solution samples of **CzPhONI** in various solvents (10^{-6} mol·L⁻¹) were excited at 370 nm using a NanoLED-370 as the excitation light source, and the emitted photons were detected by a TBX detector connected to a TBX-PS power supply. The UV-Vis absorption spectra were recorded on a Lambda 950 scanning spectrophotometer. All the films samples were obtained by spin-coating from corresponding chloroform solution with concentration of 20 mg/mL at a speed of 2000 rpm on quartz substrates. Cyclic voltammetry (CV) characterization was performed on a PARSTAT 2273 electrochemical workstation. The measurement was carried on a thin solid film sample in argon-purged 5×10^{-4} mol/L anhydrous acetonitrile solution with 0.1 mol/L tetrabutylammonium perchlorate as supporting electrolyte at a scanning rate of 50 mV/s. The CV system was constructed by a three-electrode electrochemical cell containing a Pt-wire working electrode, a Pt-wire counter electrode, and a Ag/AgNO₃ reference electrode (0.1 mol/L in acetonitrile). Each measurement was calibrated with an internal standard ferrocene/ferrocenium (Fc/Fc⁺) redox system.

2) Computational method

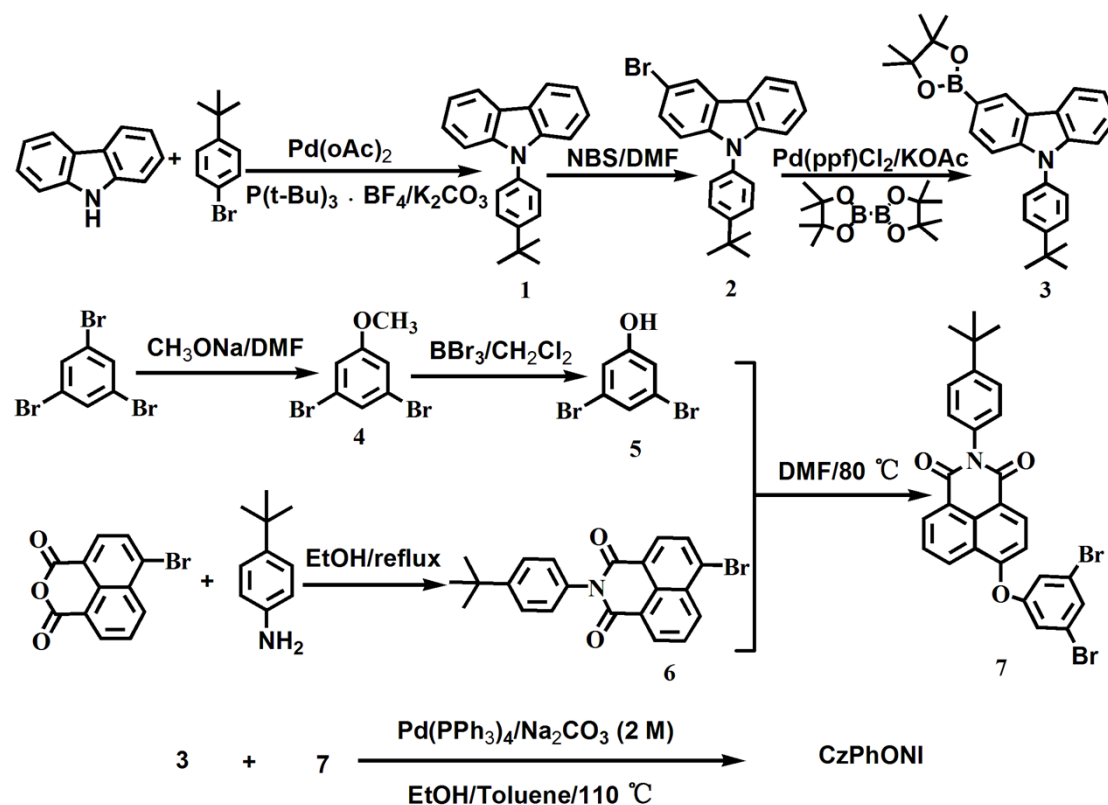
Calculations were performed using Gaussian 09 programs. The equilibrium geometry of the ground state was optimized using density functional theory (DFT) method with hybrid functional B3LYP and 6-31G(d) basis set. The solvent effect on the geometry was evaluated by means of the polarizable continuum model (PCM) incorporating toluene as the solvent.

3) OLED fabrication and measurements

Indium-tin oxide (ITO) coated glass substrate was cleaned before used and then oxygen plasma treated for 15 min. Organic functional layers were thermo-evaporated in vacuum (3×10^{-4} Pa) with a deposition rate of 0.2~0.5 Å/ s. Finally, metallic cathode was deposited with rate of 3~5 Å/ s at 3×10^{-3} Pa. The active area of the OLEDs is 2×2.5 mm². EL spectra and Commission Internationale de l'Eclairage (CIE) coordinates were recorded on an OPT-2000 instrument. Immediately after the sample preparation, the current density-voltage-luminance (*J-V-L*) characteristics of OLEDs were measured with a Keithley 2400 and an ST-86LA luminance meter, and the EL spectra were obtained by the PR650 SpectraColorimeter. For the MEL measurements, the magnetic field with maximum strength of 200 mT was applied parallel to the device surface (perpendicular to the current direction). A Keithley 2612 SourceMeter was used to provide the voltage bias from one channel and simultaneously recorded the current signals. The other channel of Keithley 2612 was used to record the EL intensity of the OLEDs collected by an optic fiber connected to a highly sensitive Hamamatsu photomultiplier (H5738-01). During the test, the photomultiplier was placed far away from the electromagnet to make sure there is no magnetic field dependence on its output. The resolution of MEL response is tested to be 0.01%. In this method, the EL signals before and after the subjection to the magnetic field were recorded, to calculate the average value of the zero-field signals. The magnetic field effects in EL are obtained by $MEL = \Delta EL / EL = (EL(B) - EL(aver, 0)) / EL(aver, 0)$. All the measurements were carried out in ambient atmosphere without encapsulation. The η_{ext} s of these three devices were calculated with a computer program on the basis of previous reported literature.³

The mobility of **CzPhONI** was estimated from the two single carrier devices based on the space charge limited current (SCLC) method and I-V characteristics of these single carrier devices according to literature.⁴ The electron-only device had a structure of Al/LiF/CzPhONI (40 nm)/LiF/Al; while the hole-only device had a structure of ITO/MoO₃/CzPhONI (40 nm)/MoO₃/Al.

4) Synthetic procedures and characterization data.



Synthetic routes to **CzPhONI**.

Synthesis of 9-(4-*t*-butylphenyl)-9*H*-carbazole (**1**)⁵

A flask was charged with carbazole (4.7 g, 28.0 mmol), 1-bromo-4-*t*-butylbenzene (5.0 g, 23.5 mmol), Pd(OAc)₂ (0.106 g, 0.47 mmol), P(*t*-Bu)₃·BF₄ (0.27 g, 0.94 mmol), K₂CO₃ (6.48 g, 47.0 mmol), and 80 mL toluene. The reaction was heated in an oil bath at 120 °C for 14 h under argon. The reaction mixture was cooled down, then poured into 150 mL water and extracted with 50 mL × 3 of CH₂Cl₂, washed with brine, and dried over anhydrous Na₂SO₄. Then the solvent was removed in vacuum, and the crude product was purified by column chromatography over silica using petroleum ether as eluent, followed by recrystallization from EtOH to afford the pure product as white needle solid. Yield: 70.8%. M.p.: 182-184 °C. ¹H NMR (400 MHz, CDCl₃) δ (ppm): 8.15 (d, *J* = 7.6 Hz, 2H), 7.61 (d, *J* = 8.0 Hz, 2H), 7.49 (d, *J* = 8.0 Hz, 2H), 7.44 (q, 4H), 7.29 (d, *J* = 6.8 Hz, 2H), 1.42 (s, 9H).

Synthesis of 3-bromo-9-(4-*t*-butylphenyl)-9*H*-carbazole (2)

A solution of N-Bromosuccinimide (2.58 g, 14.5 mmol) in DMF (80 mL) was added slowly to a solution of **1** (4.34 g, 14.5 mmol) in 150 mL DMF at 0 °C. The mixture was stirred for 24 h, then quenched with water. The precipitate was collected, washed with water and dried, then recrystallized from EtOH to afford the pure product as white solid. Yield: 80.3 %. M.p.: 142-144 °C. ¹H NMR (400 MHz, CDCl₃) δ (ppm): 8.24 (s, 1H), 8.09 (d, *J* = 7.6 Hz, 1H), 7.61 (d, *J* = 8.0 Hz, 2H), 7.47-7.40 (m, 5H), 7.29-7.28 (m, 2H), 1.42 (s, 9H).

Synthesis of 9-(4-*t*-butylphenyl)-3-(4,4,5,5-tertamethyl-1,3,2-dioxaborolan -2-yl)-9*H*-carbazole (3)

2 (5.0 g, 13.2 mmol), bis(pinacolato)diboron (3.69 g, 14.52 mmol), KOAc (3.89 g, 39.65 mmol), Pd(ppf)Cl₂ (0.2906 g, 0.4 mmol), and 100 mL of argon degassed 1,4-dioxane were added in a flask. After stirring at 100 °C for 16 h under argon, the mixture was cooled down, poured into 150 mL water, extracted with 50 mL × 3 of CH₂Cl₂, washed with brine, and dried over anhydrous Na₂SO₄. Then the solvent was removed in vacuum, and the crude material was purified by column chromatography over silica using petroleum ether/CH₂Cl₂ (4/1) as eluent to afford the pure product as white solid. Yield: 50.1 %. M.p.: 178-179 °C. ¹H NMR (400 MHz, CDCl₃) δ (ppm): 8.64 (s, 1H), 8.18 (d, *J* = 8.0 Hz, 1H), 7.86 (d, *J* = 8.0 Hz, 1H), 7.61 (d, *J* = 8.4 Hz, 2H), 7.47 (d, *J* = 8.4 Hz, 2H), 7.40-7.38 (m, 3H), 7.28 (t, 1H), 1.42 (d, 9H), 1.25 (s, 12H).

Synthesis of 3, 5-dibromoanisole (4) ⁶

A mixture of 1,3,5-tribromobenzene (5.0 g, 15.9 mmol) and CH₃ONa (1.08 g, 20.0 mmol) were added into 100 mL of anhydrous and argon degassed DMF. The reaction mixture was stirred at 80 °C for 28 h under argon. After cooled down, the mixture was quenched with 5 % aqueous hydrochloric acid, extracted with 50 mL × 3 of ethyl acetate, washed with brine, and dried over anhydrous Na₂SO₄. After removal of solvent, the crude material was purified by column chromatography over silica

using petroleum ether as eluent to afford the pure product as white solid. Yield: 48.9 %. M.p.: 34-39 °C.

Synthesis of 3,5-dibromophenol (5) ⁶

BBr₃ (1.3 mL) was added to a solution of **4** (1.0 g, 3.76 mmol) in CH₂Cl₂ (35 mL). The reaction mixture was stirred at 40 °C for 8 h. After cooled down, the mixture was quenched with 5 % aqueous hydrochloric acid in an ice water bath carefully, extracted with 20 mL × 3 of ethyl acetate, washed with brine, and dried over anhydrous Na₂SO₄. After removal of solvent, the residue was purified by column chromatography over silica using petroleum ether/ethyl acetate (15/1) as eluent to afford the pure product as white solid. Yield: 73.6 %. M.p.: 78-80 °C.

Synthesis of 4-bromo-*N*-(4-*t*-butylphenyl)-1,8-naphthalimide (6)

A flask was charged with 4-bromo-1,8-naphthalic anhydride (5.0 g, 18.05 mmol), 4-*t*-butylphenylamine (3.23 g, 21.64 mmol) and 150 mL EtOH. The reaction mixture was refluxed for 3 days under argon. After cooled down to room temperature, the solvent was removed in vacuum to afford the crude product, which was recrystallized from ethyl acetate to afford the pure product as white needle solid. Yield: 81.1 %. M.p.: 292-293 °C. ¹H NMR (400 MHz, CDCl₃) δ (ppm): 8.71 (dd, *J* = 7.2, 0.8 Hz, 1H), 8.65 (dd, *J* = 8.4, 0.8 Hz, 1H), 8.47 (d, *J* = 8.0 Hz, 1H), 8.09 (d, *J* = 7.6 Hz, 1H), 7.91 (t, *J*₁ = 7.2 Hz, *J*₂ = 8.4 Hz, 1H), 7.57 (d, *J* = 8.8 Hz, 2H), 7.24 (d, *J* = 8.8 Hz, 2H), 1.38 (s, 9H).

Synthesis of 4-(3,5-dibromophenoxy)-*N*-(4-*t*-butylphenyl)-1,8-naphthalimide (7)

A flask was charged with **5** (0.48 g, 1.9 mmol), **6** (0.5 g, 1.23 mmol), K₂CO₃ (0.29 g, 2.1 mmol) and 30 mL DMF. The reaction mixture was heated at 80 °C for 4 h under argon. After cooled down to room temperature, the mixture was poured into 150 mL water. The precipitate was filtered, washed with water, then dried in vacuum, followed by recrystallization from EtOH to afford the pure product as yellow solid. Yield: 65 %. M.p.: 274-276 °C.

Synthesis of 6-{3,5-Bis-[9-(4-*t*-butylphenyl)-9*H*-carbazol-3-yl]-phenoxy}-2-(4-*t*-

butylphenyl)-benzo[de]isoquinoline-1,3-dione (CzPhONI)

A flask was charged with **3** (0.81 g, 1.91 mmol), **7** (0.5 g, 0.87 mmol), Pd(PPh₃)₄ (0.03 g, 0.026 mmol), Na₂CO₃ (2 M, 26 mL), EtOH (26 mL) and toluene (40 mL). The reaction mixture was stirred at 110 °C for 24 h under argon. After cooled down to room temperature, the mixture was poured into 150 mL water, extracted with 50 mL × 3 of CH₂Cl₂, washed with brine, and dried over anhydrous Na₂SO₄. After removal of solvent, the crude product was purified by column chromatography over silica using petroleum ether/CH₂Cl₂ (4/1) as eluent, followed by recrystallization from CH₂Cl₂/CH₃OH for three times to yield the pure product as pale-yellow solid. Yield: 46.6 %. ¹H NMR (400 MHz, CDCl₃) δ (ppm): 8.89 (d, *J* = 8.4 Hz, 1H), 8.74 (d, *J* = 7.2 Hz, 1H), 8.58 (d, *J* = 8.0 Hz, 1H), 8.45 (s, 2H), 8.21 (d, *J* = 7.6 Hz, 2H), 8.01 (s, 1H), 7.88 (t, *J*₁ = *J*₂ = 8.0 Hz, 1H), 7.75 (dd, *J* = 8.4, 0.8 Hz, 2H), 7.64 (d, *J* = 8.4 Hz, 4H), 7.56-7.50 (m, 10H), 7.46-7.40 (m, 4H), 7.32-7.28 (m, 2H), 7.26 (s, 1H), 7.24 (s, 2H), 1.43 (s, 18H), 1.37 (s, 18H). ¹³C NMR (100 MHz, CDCl₃) δ (ppm): 164.84, 164.18, 160.48, 155.81, 151.39, 150.79, 145.21, 141.68, 140.97, 134.82, 133.52, 132.85, 132.44, 132.21, 130.27, 129.11, 128.11, 126.73, 126.63, 126.52, 126.38, 125.43, 124.27, 124.02, 123.72, 123.34, 122.98, 120.52, 120.20, 119.07, 117.63, 116.80, 111.07, 110.49, 110.29, 34.95, 34.87, 31.56, 31.51. FT-IR (KBr, cm⁻¹): 3046 (Ar, C-H), 2960 (CH₃, C-H), 2905 (CH₃, C-H), 2860 (CH₃, C-H), 1708 (C=O). TOF-MS: *m/z* 1038.4614 (M + Na⁺); calcd for (M + Na⁺): 1038.4611.

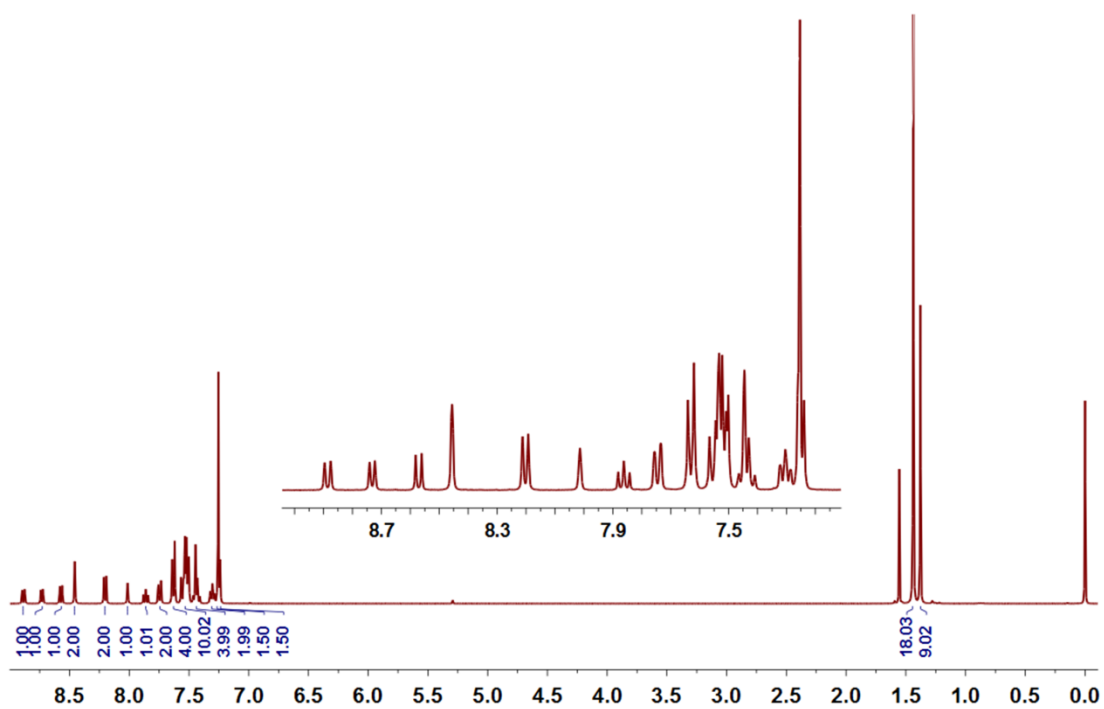
References

1. K. A. Zachariasse, S. I. Druzhinin, W. Bosch and R. Machinek, *J. Am. Chem. Soc.*, 2004, **126**, 1705.
2. Y. Wang, X. Zhang, B. Han, J. Peng, S. Hou, Y. Huang, H. Sun, M. Xie and Z. Lu, *Dyes and Pigments*, 2010, **86**, 190.
3. S. Okamoto, K. Tanaka, Y. Izumi, H. Adachi, T. Yamaji and T. Suzuki, *Jpn. J. Appl. Phys.*, 2001, **40**, 783.
4. P. W. M. Blom, M. J. M. de Jong and J. J. M. Vleggaar. *Appl. Phys. Lett.*, 1996, **68**, 3308.
5. K.-T. Wong, Y.-M. Chen, Y.-T. Lin, H.-C. Su and C.-C. Wu, *Org. Lett.*, 2005, **7**,

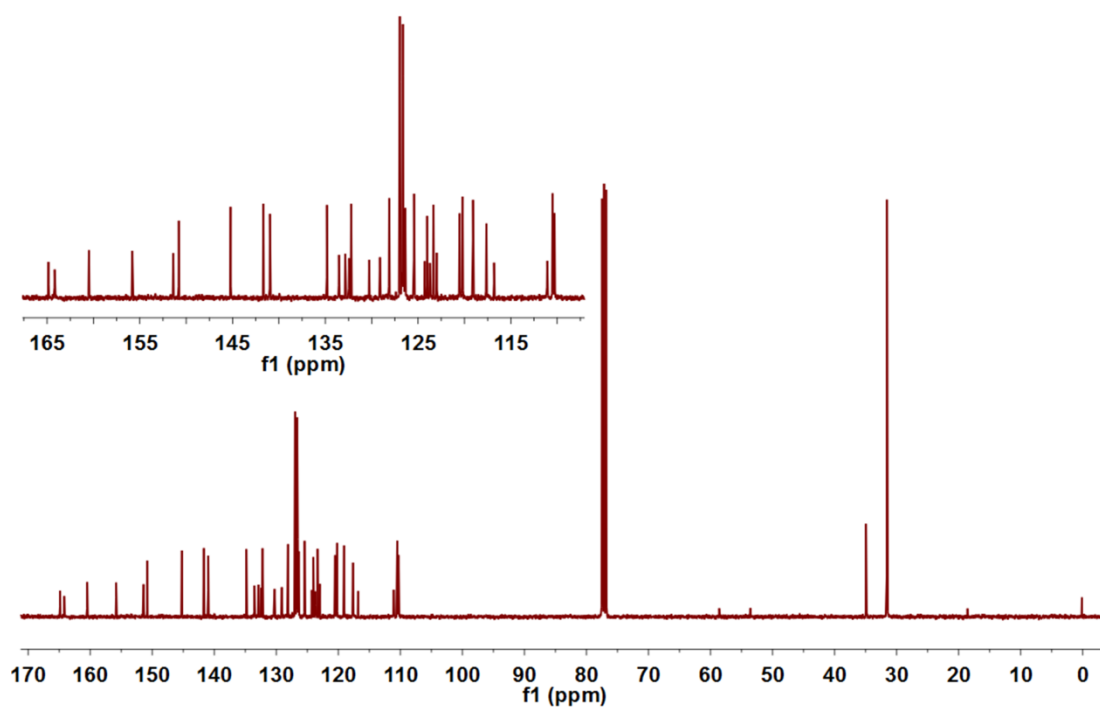
5361.

6. S. Tisserand, R. Baati, M. Nicolas and C. Mioskowski, *J. Org. Chem.*, 2004, **69**, 8982.

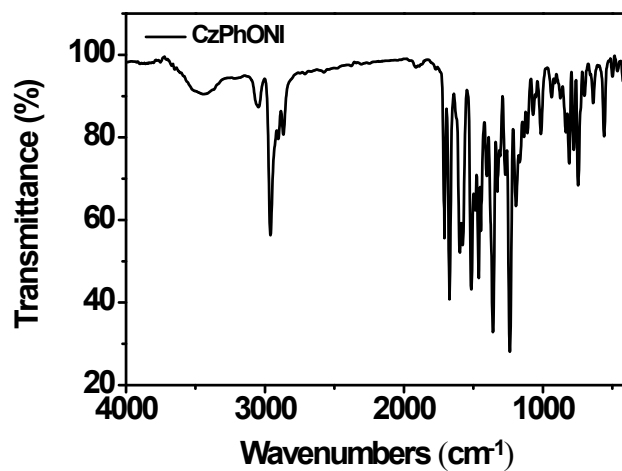
3 ^1H NMR, ^{13}C NMR, FT-IR and HRMS spectra of CzPhONI



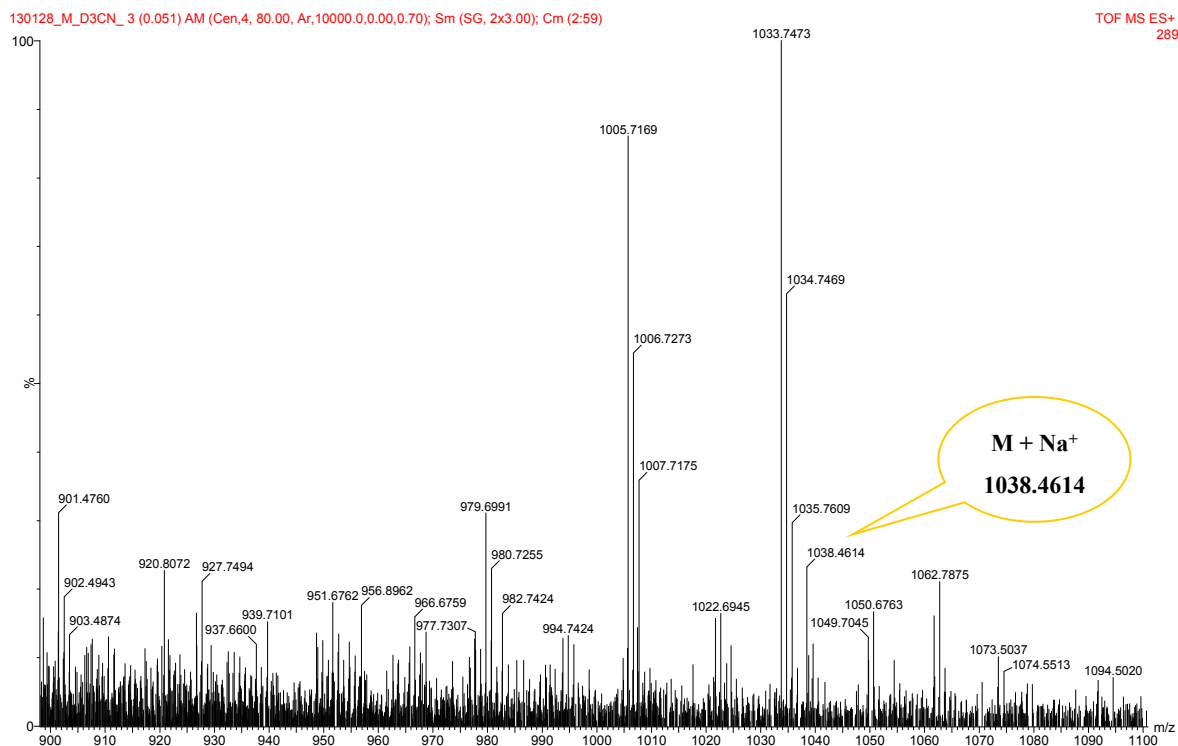
^1H NMR spectrum of CzPhONI



^{13}C NMR spectrum of CzPhONI



FT-IR spectrum of **CzPhONI**



ESI-MS spectrum of **CzPhONI**